

ARTICLE

Received 15 Oct 2012 | Accepted 8 Mar 2013 | Published 16 Apr 2013

DOI: 10.1038/ncomms2724

Dynamin–SNARE interactions control *trans*-SNARE formation in intracellular membrane fusion

Kannan Alpadi¹, Aditya Kulkarni¹, Sarita Namjoshi¹, Sankaranarayanan Srinivasan¹, Katherine H. Sippel¹, Kathryn Ayscough², Martin Zieger³, Andrea Schmidt³, Andreas Mayer³, Michael Evangelista¹, Florante A. Quiocho¹ & Christopher Peters¹

The fundamental processes of membrane fission and fusion determine size and copy numbers of intracellular organelles. Although SNARE proteins and tethering complexes mediate intracellular membrane fusion, fission requires the presence of dynamin or dynamin-related proteins. Here we study these reactions in native yeast vacuoles and find that the yeast dynamin homologue Vps1 is not only an essential part of the fission machinery, but also controls membrane fusion by generating an active Q_a SNARE-tethering complex pool, which is essential for *trans*-SNARE formation. Our findings provide new insight into the role of dynamins in membrane fusion by directly acting on SNARE proteins.

¹Verna and Marrs McLean Department of Biochemistry and Molecular Biology, Baylor College of Medicine, Houston, Texas 77030, USA. ²Department of Molecular Biology and Biotechnology, University of Sheffield, Western Bank, Sheffield S10 2TN, UK. ³Département de Biochimie, Université de Lausanne, CH-1066 Epalinges, Switzerland. Correspondence and requests for materials should be addressed to C.P. (email: cpeters@bcm.edu).

Both size and copy number of intracellular organelles can alter in reproducible ways upon changes in environmental conditions or in response to the cell cycle. Examples of these organelles include endosomes, lysosomes, vacuoles and mitochondria^{1–3}. Critical for the determination of the organelle size is the magnitude of ongoing fusion and fission reactions, which must be tightly regulated. Membrane fusion in the endomembrane system involves cognate sets of v- (vesicular or R) and t- (target or Q_a, Q_b and Q_c) SNAREs. SNAREs from two fusing membranes form *trans*-complexes between the membranes^{4–7}. Many tethers, like the vacuolar homotypic fusion and vacuole protein sorting (HOPS) complex, physically interact with SNAREs and may stimulate the formation of *trans*-SNARE complexes by bringing the opposing membranes in closer contact^{8,9}. In addition to tethering complexes, many other proteins have been identified to interact with SNAREs, including Munc13, V-ATPase, dynamins, complexins, synaptotagmins and Sec1/Munc18 proteins^{10,11}. How these proteins help to coordinate the SNARE-mediated fusion process with the antagonistic membrane fission reaction is an area that has remained unexplored.

It is not clear whether the fission machinery for different organelles is related, or fission occurs in unique, organelle-specific ways. One potential common factor is dynamin-like GTPases, which are important for vacuolar and mitochondrial fission^{2,3}. Under suitable conditions, dynamins form spiral- or ring-like collars on artificial liposomes, leading to their tubulation and fragmentation upon GTP hydrolysis^{12–14}. The GTPase effector domain and the middle domain of dynamin have been shown to be needed for self-assembly and allosteric regulation of the GTPase activity^{13,15}. Interestingly, recent studies have revealed the involvement of dynamin in granular exocytosis¹⁶. In an earlier study, we showed a dual function of the dynamin-like protein, Vps1, in membrane fission and fusion¹⁷; however, the underlying molecular mechanism allowing Vps1 to regulate both processes has remained unexplored. Here we investigate the molecular mechanism of how Vps1 controls membrane fusion and coordinates fusion with the antagonistic fission process.

Results

Vps1 controls *trans*-SNARE formation. Vacuoles purified from *vps1Δ* strains are fusion incompetent¹⁷. In contrast to pure *vps1Δ* fusions, mixed fusions employing wild-type and *vps1Δ* vacuoles displayed considerable fusion activity (~50% of wild-type levels, Fig. 1a). Fusion efficiency was determined by measuring alkaline phosphatase activity; pro-alkaline phosphatase in the BJ vacuoles is activated by maturation enzymes contained in DKY vacuoles¹⁷. As *trans*-SNARE complex formation is essential for successful fusion, we asked first whether the absence of *trans*-SNARE formation accounts for the fusion defect of *vps1Δ* vacuoles. Yeast vacuoles harbour four SNAREs that are required for their fusion¹⁸. The Q_a SNARE Vam3, the Q_b SNARE Vti1, the Q_c SNARE Vam7 and the R-SNARE Nyv1 form the *trans*-SNARE complexes necessary for fusion. A characteristic feature of vacuolar fusion is its homotypic architecture, meaning that both fusion partners harbour the same SNARE composition on their respective surfaces¹⁸. To analyse the *trans*-SNARE complex formation, we tagged either Nyv1 or Vam3 on wild-type and *vps1Δ* vacuoles. Addition of the haemagglutinin (HA) or vesicular stomatitis virus (VSV) tag to the carboxy terminus did not impair SNARE function (Supplementary Fig. S1A). Priming and docking occur in the presence of ATP. Accordingly, no *trans*-SNARE interactions were detectible in the absence of ATP. When Vam3-HA was precipitated from wild-type vacuoles in the presence of ATP, Nyv1-VSV co-precipitated from wild-type vacuoles, indicating that normal *trans*-SNARE formation had

occurred (Fig. 1a). However, when Vam3-HA was precipitated from *vps1Δ* vacuoles, no co-precipitating Nyv1-VSV could be detected, suggesting that Vps1 might be an essential factor for successful *trans*-SNARE formation.

An earlier study showed that Vps1 controls Vam3 function¹⁷. Moreover, mixed fusions between wild-type and *vps1Δ* vacuoles retained 50% of fusion activity (Fig. 1a), suggesting that not all SNAREs are functionally affected by the *vps1Δ* mutation. Therefore, we asked what topology of *trans*-SNARE complex formation might account for the mixed fusion array. Again, when Vam3-HA was precipitated from wild-type vacuoles upon addition of ATP, Nyv1-VSV co-precipitated from wild-type vacuoles, indicating that normal *trans*-SNARE formation had occurred (Fig. 1b, top panel). However, when Vam3-HA was originating from *vps1Δ* vacuoles, Nyv1-VSV did not co-precipitate even from wild-type vacuoles (Fig. 1b, top panel). Another picture emerged when Vam3-HA was precipitated from wild-type vacuoles. In this case, Nyv1-VSV from wild-type or *vps1Δ* vacuoles was able to interact *in trans* with Vam3-HA from wild-type vacuoles (Fig. 1b, bottom panel). These data suggest that the *vps1Δ* phenotype does not lead to a general disability of all vacuolar SNAREs, but specifically hits the Q_a SNARE Vam3 in its function to enter into *trans*-SNARE complexes, further confirming the role of Vps1 in controlling Vam3 activity during membrane fusion.

Next we tested whether point mutations in Vps1 might confer defects on vacuolar fusion and the *trans*-SNARE complex formation. The K42A mutation leads to a GTP-hydrolysis-defective Vps1 protein^{19–21} and the I649 mutation affects the self-assembly of Vps1 (refs 22,23; Supplementary Fig. S1B). Vacuoles purified from these strains exhibited dramatically reduced fusion activity and, concomitantly, little or no *trans*-SNARE complex formation (Fig. 1c). These data suggest that the amount of *trans*-SNARE complex formation is directly connected to the physical state of Vps1. To promote efficient *trans*-SNARE formation, Vps1 needs to hydrolyse GTP and has to be present in a polymeric state.

The interaction of the Q_a SNARE Vam3 with HOPS requires Vps1. To further elucidate the molecular impact of Vps1 mutations on the function of Vam3 in vacuolar fusion and *trans*-SNARE establishment, we investigated the abundance of different Vam3 pools on wild-type and *vps1Δ* vacuoles. Vam3 can reside in different states on the vacuolar surface, either as a single SNARE bound to the tethering complex HOPS or interacting with the NSF/Sec18 adapter protein Sec17/α-SNAP and other SNAREs as part of vacuolar *cis*-SNARE complexes²⁴. We selectively precipitated Sec17 and Vps33 from detergent-extracted wild-type and *vps1Δ* vacuoles using antibodies specific for Sec17 or the HA extension of Vps33. Vps33 is the vacuolar SM protein and an integral part of the HOPS complex²⁵. Addition of the HA extension to the C terminus did not impair Vps33 function (Supplementary Fig. S2). We found Vps1 to be significantly enriched in the Vps33-HA fraction precipitated from wild-type detergent extracts and almost totally absent in the Sec17 pulldown (Fig. 2a). A significantly lower level of Vam3 co-precipitated with Vps33-HA in *vps1Δ* vacuoles when compared with wild-type Vps33-HA precipitations, although the total amount of precipitated Vps33 was almost equal (Fig. 2a). However, the amount of Vam3 associated with Sec17 in *vps1Δ* vacuoles was comparable to wild-type levels. This suggests that only in the presence of Vps1, Vam3 is able to interact with the HOPS complex and is not exclusively found in Sec17-associated *cis*-SNARE complexes (Fig. 2a). SNAREs must interact with the tethering complex HOPS to establish *trans*-SNARE

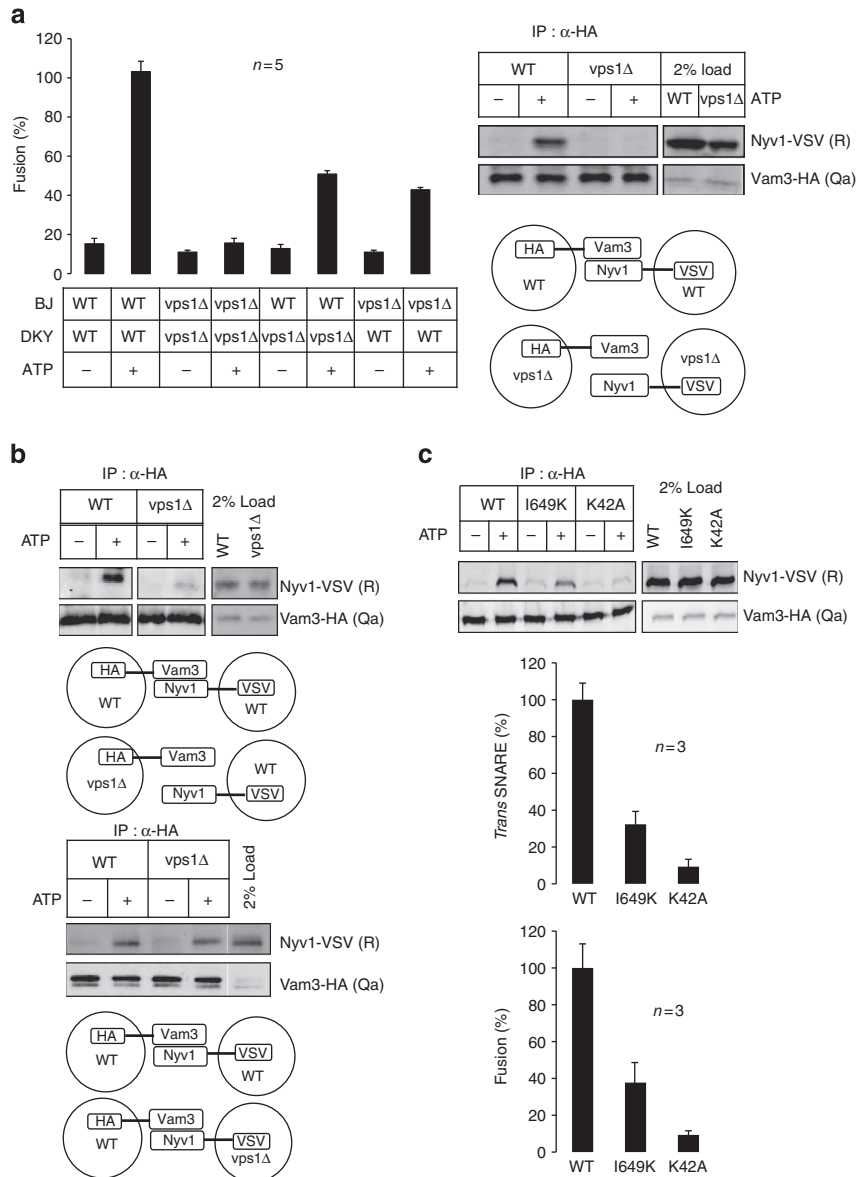


Figure 1 | Vps1 controls trans-SNARE formation. (a) Vacuoles derived from wild-type (BJ and DKY) and *vps1Δ* (BJ and DKY) strains were incubated under standard fusion condition. Mixed fusions containing wild-type and *vps1Δ* vacuoles displayed 50% fusion activity when compared with pure wild-type fusions. Five independent experiments are shown as means ± s.d. Vacuoles harbouring either Vam3-HA or Nyv1-VSV were isolated from wild-type and *vps1Δ* yeast cells. *Trans*-SNARE assays were performed as described in the Methods section. Vacuoles purified from *vps1Δ* vacuoles do not establish *trans*-SNAREs. (b) Vacuoles harbouring either Vam3-HA or Nyv1-VSV were isolated from wild-type and *vps1Δ* yeast cells. *Trans*-SNARE assays were performed as mentioned in the Methods section. In the top panel, *trans*-SNARE formation of Vam3-HA-tagged vacuoles derived from wild-type or *vps1Δ* strains with Nyv1-VSV-tagged vacuoles purified from wild-type cells are displayed. In the bottom panel, Vam3-HA tagged vacuoles from wild-type cells were mixed with wild-type or *vps1Δ* vacuoles harbouring Nyv1-VSV. On *vps1Δ* vacuoles, only the Q_a SNARE Vam3 but not the R-SNARE Nyv1 is impaired in its capability to enter into *trans*-SNARE complexes. (c) Vacuoles purified from wild-type, I649K and K42A strains harbouring Vam3-HA or Nyv1-VSV were examined for *trans*-SNARE complex formation. Means ± s.d. of three independent experiments are shown. Vacuoles purified from wild-type, I649K and K42A strains were examined for fusion activity as described in the Methods section. Three independent experiments are shown as means ± s.d.

complexes^{25–27}. We found that Vam3 is associated with the HOPS complex and Vps1 (Fig. 2b). However, the composition of this complex was changed upon addition of ATP. When Vps33-HA was precipitated from wild-type vacuoles in the presence of ATP, Vps1 was released from the Vam3–HOPS complex (Fig. 2b). Most likely, this reaction is controlled by NSF/Sec18, as temperature inactivation of this ATPase led to impaired release activity of Vps1 from the Vam3–HOPS complex (Supplementary Fig. S3). On the basis of the observation that Vps1 controls SNARE–HOPS associations and *trans*-SNARE

formation, we determined whether mutations in Vps1 might affect these interactions. We measured the Q_a-SNARE density on the HOPS complex by precipitating Vps33-HA from wild-type and mutant vacuoles. Interestingly, we detected a correlation between the extent of Vam3–HOPS coprecipitation rates and fusion efficiency (Figs. 2c, 1c). Whereas the K42A mutant exhibited rates much like the *vps1Δ* strain, the I649K mutant showed about 35% of the wild-type Vam3– coprecipitation signal, which matched the fusion efficiency of this mutant (Figs. 2c, 1c) when compared with wild type.

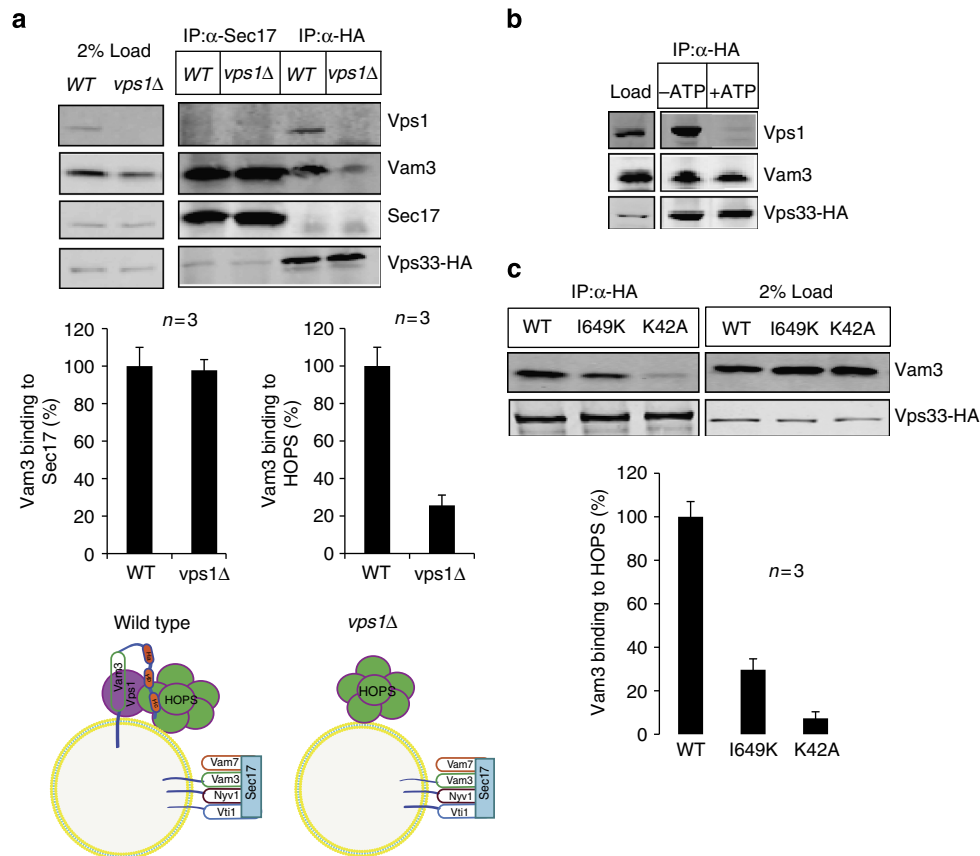


Figure 2 | The interaction of Vam3 with HOPS requires Vps1. (a) Wild-type and *vps1Δ* vacuoles were detergent extracted and immunoprecipitated either with anti Sec17 antibodies or with anti HA antibodies. Immunoprecipitation assay was done as explained in the Methods section. Vam3 binding to Sec17 and Vam3 binding to Vps33-HA were quantified using Odyssey software. Means \pm s.d. of three independent experiments are shown. The diagrammatic model displays the different Vam3-containing complexes on wild-type and *vps1Δ* vacuoles. (b) Vps1 is released from HOPS-Vam3 in the presence of ATP. Wild-type vacuoles were incubated for 15 min in the absence and presence of ATP. After detergent extraction, Vps33-HA was precipitated and co-precipitating proteins were analysed by western blotting. (c) Vacuoles purified from wild-type, K42A and I649K strains were processed as described in b. Vps33-HA was precipitated from detergent extracts and co-precipitating proteins were analysed. The band intensity was quantified from three independent experiments. Means \pm s.d. of three independent experiments are shown.

Vps1 specifically binds to the Vam3 SNARE domain. As the release activity of Vps1 from Vam3 is a prerequisite¹⁷ for successful vacuolar fusion (Fig. 2b), we asked, whether the addition of excess rVps1 might compensate for the release of endogenous Vps1 from Vam3, and hence might inhibit vacuolar fusion. We confirmed this by adding an increasing amount of rVps1 to fusion reactions ($IC_{50} \sim 1.8 \mu\text{M}$, Fig. 3a and Supplementary Fig. S4) and, moreover, addition of rVps1 ($5 \mu\text{M}$) to vacuoles completely suppressed *trans*-SNARE formation (Fig. 3b).

Having established that Vps1 controls Vam3 function during the *trans*-SNARE formation (Fig. 1b), we sought for an experimental approach, which would allow us to convincingly demonstrate the specificity of Vps1 binding towards Vam3. In addition, we were interested in what domain of Vam3 might interact with Vps1. We therefore performed dot blot experiments by immobilizing full-length Vam3, the amino-terminal Habc domain, the SNARE domain of Vam3 and full-length Nyv1 onto nitrocellulose membranes. When the immobilized proteins were exposed to rVps1, only full-length Vam3 and the SNARE domain of Vam3 exhibited binding towards Vps1 (Fig. 3c). We determined the K_d of Vam3-Vps1 interactions by biolayer interferometry using an Octet Red 96 instrument (ForteBio Inc.) at $3.63 \times 10^{-7} \text{M}$ (Supplementary Fig. S5).

To confirm that Vps1 mainly interacts with the SNARE domain of Vam3, we investigated the SNARE complex formation of recombinantly expressed SNAREs in the presence of increasing concentrations of rVps1 (Fig. 3d). We speculated that Vps1 might sequester Vam3 from the SNARE complex, leading to decreased numbers of tetrameric SNARE complexes. Indeed, in the presence of rVps1, SNARE complex formation was suppressed up to 65% (Fig. 3d).

Dynasore inhibits vacuolar fission and fusion *in vivo*. Yeast vacuoles fragment upon cellular exposure to hypertonic stress¹⁷ or at the onset of bud emergence³ as visualized by fluorescence microscopy after staining with the fluorescent dye FM4-64¹⁷. Using the hypertonic stress response, we visualized the inhibition of vacuolar fission and fusion *in vivo* by dynasore. Dynasore is a small molecule, selective non-competitive inhibitor of the protein dynamin²⁸. Logarithmic-phase yeast cells were stained with FM4-64. To first explore the effect of dynasore on vacuolar fission, we added either dynasore or the solvent dimethylsulphoxide (DMSO) to the stained cells and subsequently induced fission by a brief high-salt exposure (Fig. 4A, upper panel). DMSO did not inhibit vacuolar fragmentation as visualized by the increased

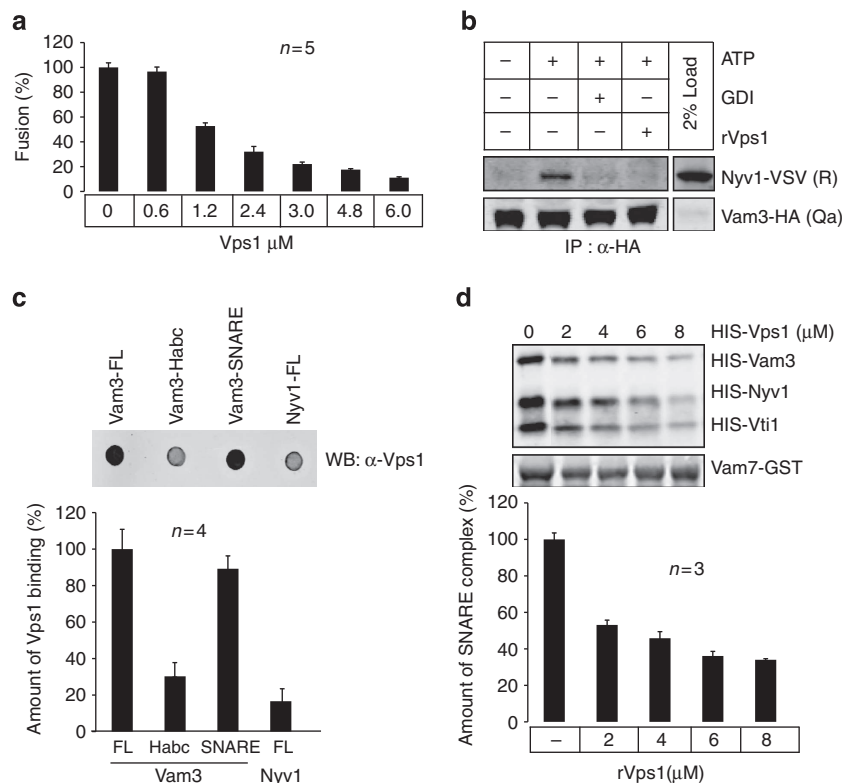


Figure 3 | Vps1 specifically binds to the Q_a SNARE Vam3. (a) Recombinant Vps1 inhibits vacuole fusion. Vacuoles derived from BJ3505 and DKY6805 strains were incubated with increasing concentration of rVps1 in standard fusion reaction as described in the Methods section. Vacuolar fusion was completely inhibited at a concentration of 6 μM rVps1. (b) Recombinant Vps1 inhibits *trans*-SNARE formation. The *trans*-SNARE assay was performed as described. Recombinant Vps1 was added to the assay at a concentration of 6 μM. GDI, which extracts the small G-protein Ypt7 from the vacuolar membrane, was added as an inhibitor of *trans*-SNARE formation at a concentration of 5 μM. At the given concentration, rVps1 suppressed *trans*-SNARE formation much like GDI. (c) Vps1 binds to the SNARE domain of Vam3. 1 μg of full-length Vam3, N-terminal domain of Vam3 (1-190), SNARE domain of Vam3 (190-252) and full-length Nyv1 were immobilized on a nitrocellulose membrane and incubated with rVps1 overnight. Detection of bound rVps1 was performed as described in the Methods section. Means ± s.d. of three independent experiments are shown. Only full-length Vam3 and the SNARE domain of Vam3 displayed binding towards rVps1. (d) Recombinant Vps1 inhibits SNARE complex formation. The indicated recombinant proteins (2 μg for all SNAREs) were incubated with increasing concentrations of rVps1 for 1 h at 4 °C and subsequently Vam7-GST was precipitated. Co-precipitating proteins were analysed using SDS-PAGE and western blotting. In the presence of 6 μM rVps1, SNARE complex formation is suppressed up to 65%. Three independent experiments are shown as means ± s.d.

number of smaller vacuoles (70% of vacuoles fragmented; Fig. 4A upper panel), whereas dynasore diminished this amount drastically (only 20% of vacuoles fragmented; Fig. 4A upper panel). To assess the *in vivo* effect of dynasore on vacuolar fusion, we fragmented the stained vacuoles by brief salt exposure and subsequently added dynasore or DMSO (Fig. 4A, lower panel). After release of the vacuoles from the hypertonic media, vacuoles started to refuse, but this was significantly less efficient in the presence of dynasore (only 50% of the DMSO control, Fig. 4A, lower panel). Along with our *in vivo* investigations, we confirmed the inhibitory effect of dynasore on vacuole fusion and *trans*-SNARE formation *in vitro*. In the presence of 100 μM dynasore, we could not observe any *trans*-SNAREs formation and vacuolar fusion (Fig. 4B). The GTPase activity of rVps1 was inhibited up to 60% by dynasore (Fig. 4C). These data indicate that Vps1 function is critical for controlling vacuolar fission and fusion.

Discussion

We have demonstrated that Vps1 is an essential factor in vacuolar fusion. In the absence of Vps1, as well as in the presence of excess rVps1, vacuolar fusion and *trans*-SNARE establishment are impaired. We interpret the data as a two step process. First,

Vps1 induces a population of Vam3 that associates with HOPS rather than pairing with other SNAREs. Although *cis*-SNARE complexes can be considered as a reservoir for single SNAREs dependent on activation through Sec18/NSF, the HOPS-associated fraction of Vam3 is likely essential for organizing SNARE nucleation and *trans*-SNARE formation^{27,29}. Our data suggest that the population of HOPS-associated Vam3 is absent on *vps1Δ* vacuoles. As Vps1 predominantly interacts with the SNARE domain of Vam3, it prevents the formation of SNARE complexes in the initial phase of membrane fusion. Consequently, to initiate SNARE nucleation and *trans*-SNARE interactions, Vps1 has to be released from Vam3¹⁷. Addition of excess recombinant Vps1 impairs this process and inhibits vacuolar fusion and *trans*-SNARE formation, emphasizing the importance of the release event.

A second function of Vps1 might be the control of SNARE density with the tethering complex HOPS. Vps1 might actively increase SNARE density at the contact site of two fusing membrane by recruiting several Q_a SNAREs to the tethering complex (Fig. 4D). Dynamin with its tendency to polymerize under the appropriate conditions and with its ability to interact with SNARE proteins is likely to be an important regulator of SNARE complex density at the fusion site.

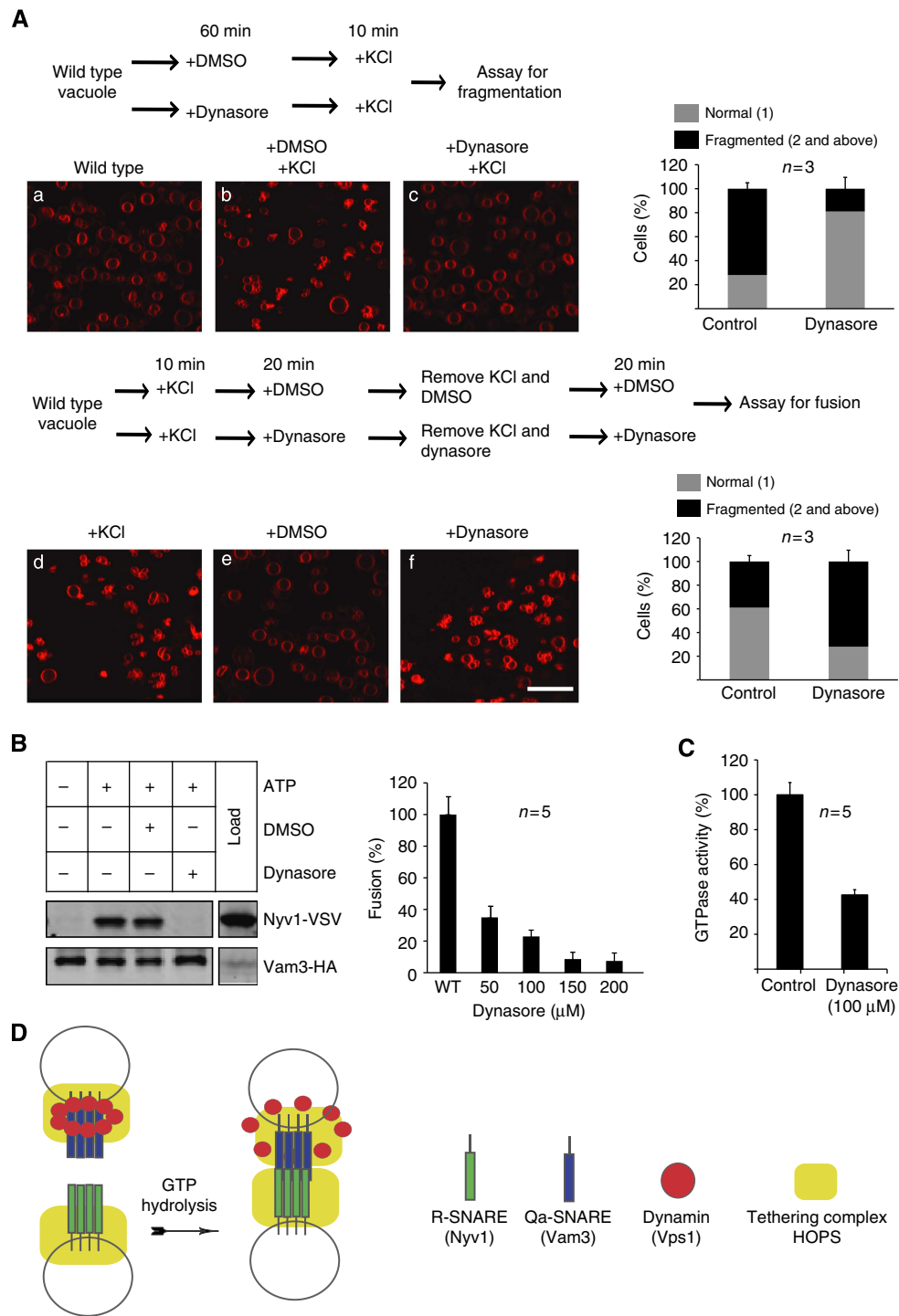


Figure 4 | Dynasore inhibits vacuolar fission and fusion *in vivo*. **(A)** Vacuoles of wild-type yeast cells were labelled with FM4-64 using the standard procedure as described in the Methods section. In the assay for fragmentation, (a) shows the normal vacuole structure of logarithmic phase wild-type cells, (b) shows salt-induced fragmentation of vacuoles in the presence of solvent DMSO. (c) Salt-induced phenotype of vacuoles in the presence of 100 μ M dynasore. The percentage of cells showing normal or fragmented vacuoles was quantified. One hundred cells were counted randomly in each experiment. Three independent experiments are shown as means \pm s.d. In the assay for fusion (d) shows the fragmented vacuoles after salt exposure; (e) shows the effect of the solvent DMSO on re-fusion of fragmented vacuoles; (f) displays the influence of dynasore on re-fusion of fragmented vacuoles. The percentage of cells exhibiting normal or fragmented vacuoles was quantified. One hundred cells were counted randomly in each experiment. Three independent experiments are shown as means \pm s.d. Scale bar 5 μ m. **(B)** Dynasore at a concentration of 100 μ M inhibits *in vitro* vacuole fusion and *trans*-SNARE complex formation. **(C)** Dynasore inhibits the GTPase activity of recombinant Vps1. **(D)** Model explaining the role of Vps1 in *trans*-SNARE formation. Vps1 in its polymeric state recruits multiple Q_a-SNAREs to the tether HOPS. As Vps1 is bound to the SNARE domain of Vam3, it has to be released before the formation of *trans*-SNAREs. After GTP hydrolysis and concomitant Vps1 release have occurred, multiple *trans*-SNAREs form at the fusion site. In the absence of Vps1 or in the presence of mutations in Vps1 leading to defects in GTP hydrolysis or polymerization, the number of formed *trans*-SNAREs does not reach the necessary threshold at the fusion site to promote complete membrane fusion.

This is supported by our data showing that in the GTPase- and polymerization-deficient Vps1 mutants K42A and I649K, the amount of HOPS-associated Vam3 and extent of *trans*-SNARE formation is significantly lower compared with wild type.

Currently, there is ample discussion about the exact number of *trans*-SNARE complexes needed to promote full content mixing between two fusing membranes, varying between one and four³⁰. On the basis of our observations made in the I649K Vps1 mutant, we prefer the idea of multiple *trans*-SNARE complexes per fusion site to promote full membrane bilayer merging.

Methods

Vacuole isolation. Vacuoles were isolated as described previously¹⁷. DKY6281 and BJ3505 strains carrying tagged SNAREs were grown in Yeast extract Peptone Dextrose (YPD) at 30 °C at 225g to optical density (OD)₆₀₀ = 2 and were collected (3 min, 5,000g). Vacuoles were isolated through hydrolysing yeast cell walls using lyticase³¹, recombinantly expressed in *Escherichia coli* RSB805 (provided Dr Randy Schekman, Berkeley), and were prepared from a periplasmic supernatant. Collected cells were resuspended in reduction buffer (30 mM Tris/Cl pH 8.9, 10 mM dithiothreitol (DTT)) and incubated for 5 min at 30 °C. After collecting the cells as described above, they were resuspended in 15 ml digestion buffer (600 mM sorbitol, 50 mM K-phosphate pH 7.5 in Yeast extract Peptone (YP) medium with 0.2% glucose and 0.1 mg ml⁻¹ lyticase preparation). After 20 min at 30 °C, cells were centrifuged (1 min 5,800g in JLA25.5 rotor). The spheroplasts were resuspended in 2.5 ml 15% Ficoll-400 in PS buffer (10 mM PIPES/KOH Sorbitol buffer pH 6.8, 200 mM sorbitol) and 200 µl DEAE-dextran (0.4 mg ml⁻¹ in PS). After 90 s of incubation at 30 °C, the cells were transferred to SW41 tubes and overlaid with steps of 8, 4 and 0% Ficoll-400 in PS. Cells were centrifuged for 75 min at 2 °C and 30,000g in a SW41 rotor.

Vacuole fusion. *In vitro* vacuole fusion assay was carried out as described previously¹⁷. In brief, DKY6281 and BJ3505 vacuoles were adjusted to a protein concentration of 0.5 mg ml⁻¹ and incubated in a volume of 30 µl PS buffer (10 mM PIPES/KOH pH 6.8, 200 mM sorbitol) with 125 mM KCl, 0.5 mM MnCl₂, 1 mM DTT. Inhibitors were added before starting the fusion by addition of the ATP-regenerating system (0.25 mg ml⁻¹ creatine kinase, 20 mM creatine phosphate, 500 µM ATP, 500 µM MgCl₂). After 60 min at 27 °C, or on ice, 1 ml of PS buffer was added, vacuoles were centrifuged (2 min, 20,000g, 4 °C) and resuspended in 500 µl developing buffer (10 mM MgCl₂, 0.2% TX-100, 250 mM TrisHCl pH 8.9, 1 mM *p*-nitrophenylphosphate). After 5 min at 27 °C, the reactions were stopped with 500 µl 1 M glycine pH 11.5 and the OD was measured at 400 nm.

Trans-SNARE assay. Vacuoles were adjusted to a protein concentration of 0.5 mg ml⁻¹. The total volume of one assay was 1 ml containing equal amounts of the two fusion partners in PS buffer with 125 mM KCl, 0.5 mM MnCl₂ and 1 mM DTT. Mixed vacuoles were incubated for 5 min at 27 °C in the absence of ATP. The fusion reaction was started by adding ATP-regenerating system (0.25 mg ml⁻¹ creatine kinase, 20 mM creatine phosphate, 500 µM ATP, 500 µM MgCl₂). After 30 min at 27 °C, the vacuoles were centrifuged for 2 min at 4 °C at 20,000g. The pellet was resuspended in 1.5 ml solubilization buffer (0.5% Triton, 50 mM KCl, 3 mM EDTA, 1 mM DTT in PS). After centrifugation for 4 min at 4 °C (20,000g), the supernatant was incubated with 30 µl Protein G beads (Roche) and 15 µg HA-antibodies (Covance, mouse monoclonal) for 1 h at 4 °C with gentle shaking. The Protein G beads were washed three times with 50 mM KCl, 0.25% Triton, 3 mM DTT and 3 mM EDTA in PS buffer, and incubated for 5 min at 60 °C in 2 × reducing SDS sample buffer.

In vivo fragmentation and re-fusion assay. Logarithmic grown BJ3505 cells were stained with FM4-64 (10 µM) for 30 min at 30 °C in YPD and subsequently chased for another 60 min. To visualize dynasore's effect on fragmentation, stained cells were incubated for 1 h in YPD in the presence of 100 µM dynasore. Thereafter, cells were briefly centrifuged and further incubated in YPD supplemented with 200 mM KCl and 100 µM dynasore. After 10 min cells were inspected for fragmentation using fluorescence confocal microscopy. To investigate dynasore's impact on fusion, stained cells were first fragmented by a brief incubation in YPD containing 400 mM KCl (10 min). Dynasore then was added at a concentration of 100 µM, and cells were incubated for a further 10 min in the high-salt YPD. Afterwards, cells were briefly centrifuged and released from the osmotic pressure by addition of normal YPD containing 100 µM dynasore. After 20 min, cells were inspected for re-fusion of fragmented vacuoles using fluorescence confocal microscopy.

HOPS precipitation assay. Vacuoles were isolated from BJ3505 wild-type and vps1Δ strains harbouring Vps33-HA. Two milligram of vacuoles purified from each strain were incubated with or without ATP in PS buffer containing 100 mM KCl and 500 µM MnCl₂ for 15 min at 27 °C. Subsequently, the vacuoles were solubilized in buffer containing 100 mM KCl, 500 µM MnCl₂ and 0.3% TritonX-100.

The samples were centrifuged at 20,000g for 10 min, and 10 µg of HA antibody (Covance) and Protein G beads were added to the solubilizate. After incubation for 1 h at 4 °C with end-to-end rotation, the samples were centrifuged for 1 min and the beads were washed twice with solubilization buffer. SDS sample buffer was added to the beads and incubated at 90 °C for 2 min. The eluted proteins were separated by SDS-PAGE and analysed by western blotting with the indicated antibodies.

GST-pulldown assay. Nyv1, Vam3 and Vti1 were expressed as full-length proteins devoid of the transmembrane domain from pET28 vectors harbouring a poly-His tag on their N terminus. Vam7 was expressed from a pGEX vector as a N-terminally tagged GST protein. Vps1 was expressed as a full-length protein harbouring a poly-His tag on the N terminus². A solution containing 2 µg each of GST-Vam7, His-Vam3, His-Vti1 and His-Nyv1 was incubated for 1 h at 4 °C, with various amounts of His-Vps1 in PS buffer with 100 mM KCl and 1 mM DTT in the presence of glutathione beads. Thereafter, samples were briefly centrifuged and washed three times using the same buffer. Following, 2 × concentrated reducing SDS sample buffer was added to the beads and precipitated proteins were analysed using SDS-PAGE and western blotting.

Dot blot assay. Vam3 proteins were expressed as full-length, N-terminal domain and SNARE domain from pTYB12 vector with an intein tag on the N terminus. Vam3 full-length (1–252), the N-terminal domain (1–190) and the SNARE domain (190–252) were cloned into a pTYB12 vector using *SpeI* and *XhoI* sites. Proteins were purified as recommended in the IMPACT manual (New England Biolabs). Briefly, BL21(DE3) cells transformed with the plasmid were induced at OD₆₀₀ of 0.8–1.0 with 0.5 mM isopropyl-β-D-thiogalactoside at 16 °C overnight and bound to chitin beads after cell lysis in 20 mM HEPES, 500 mM NaCl, pH 8.0. On-column cleavage was performed for 16 h at room temperature in the same buffer, with the addition of 50 mM DTT. This was dialysed with 20 mM Tris-HCl, 50 mM NaCl, pH 7.0. Vps1 was expressed as His-Vps1 was purified, as described earlier². Vam3 samples (1 µg) were applied to a nitrocellulose membrane and blocked with 5% skim milk for 1 h at room temperature. Vps1 at a concentration of 10 µg ml⁻¹ in 5% skim milk was added to the membrane and incubated overnight at 4 °C. The membrane was washed with PBS for 5 min and incubated with anti-Vps1 antibodies for 1 h at room temperature. Subsequently, the membrane was washed with PBS for 5 min and incubated with anti-rabbit secondary antibodies.

GTPase assay. GTP hydrolysis was followed by monitoring release of P_i, which was quantified by a colorimetric method as described³². For basal GTPase assays, Vps1 was diluted to 1 µM in GTPase assay buffer (20 mM HEPES-KOH pH 7.5, 150 mM KCl, 2 mM MgCl₂, 1 mM DTT). Vps1 was incubated with dynasore at a concentration of 100 µM for 20–30 min at room temperature with shaking. The inhibitor stock was freshly prepared at a final concentration of 3 mM in DMSO. GTP was added to the samples at a final concentration of 1 mM and incubated at 37 °C for 15 min with shaking. The reactions were stopped with 100 mM EDTA, pH 8.0. The free orthophosphate was measured using a malachite green phosphate assay kit (Bioassay System).

Microscopy. Images were taken from a Leica TCS SP5 confocal microscope using an argon laser. Images were exported as TIFF files. Images were cropped from TIFF files and pasted into Adobe Illustrator CS3. The final figure file was saved as adobe illustrator (.ai) format.

Western blot images. The western blot images were taken from a LI-COR Odyssey Infrared Imager. The files were exported as TIFF and processed in adobe illustrator CS3. The band intensity was quantified using densitometry software supplied with the Odyssey Infrared Imager.

References

- Luzio, J. P., Pryor, P. R. & Bright, N. A. Lysosomes: fusion and function. *Nat. Rev. Mol. Cell Biol.* **8**, 622–632 (2007).
- Okamoto, K. & Shaw, J. M. Mitochondrial morphology and dynamics in yeast and multicellular eukaryotes. *Annu. Rev. Genet.* **39**, 503–536 (2005).
- Weisman, L. S. Organelles on the move: insights from yeast vacuole inheritance. *Nat. Rev. Mol. Cell Biol.* **7**, 243–252 (2006).
- Pelham, H. R. SNAREs and the specificity of membrane fusion. *Trends Cell Biol.* **11**, 99–101 (2001).
- Weber, T. *et al.* SNAREpins: minimal machinery for membrane fusion. *Cell* **92**, 759–772 (1998).
- Ungermann, C., Sato, K. & Wickner, W. Defining the functions of *trans*-SNARE pairs. *Nature* **396**, 543–548 (1998).
- Fukuda, R. *et al.* Functional architecture of an intracellular membrane t-SNARE. *Nature* **407**, 198–202 (2000).
- Pieren, M., Schmidt, A. & Mayer, A. The SM protein Vps33 and the t-SNARE H(abc) domain promote fusion pore opening. *Nat. Struct. Mol. Biol.* **17**, 710–717 (2010).

9. Brocker, C., Engelbrecht-Vandre, S. & Ungermann, C. Multisubunit tethering complexes and their role in membrane fusion. *Curr. Biol.* **20**, R943–R952 (2010).
10. Galas, M. C., Chasserot-Golaz, S., Dirrig-Grosch, S. & Bader, M. F. Presence of dynamin–syntaxin complexes associated with secretory granules in adrenal chromaffin cells. *J. Neurochem.* **75**, 1511–1519 (2000).
11. Malsam, J., Kreye, S. & Sollner, T. H. Membrane fusion: SNAREs and regulation. *Cell Mol. Life Sci.* **65**, 2814–2832 (2008).
12. Pawlowski, N. Dynamin self-assembly and the vesicle scission mechanism: how dynamin oligomers cleave the membrane neck of clathrin-coated pits during endocytosis. *Bioessays* **32**, 1033–1039 (2010).
13. Schmid, S. L. & Frolov, V. A. Dynamin: functional design of a membrane fission catalyst. *Annu. Rev. Cell Dev. Biol.* **27**, 79–105 (2011).
14. Hinshaw, J. E. Dynamin and its role in membrane fission. *Annu. Rev. Cell Dev. Biol.* **16**, 483–519 (2000).
15. Ramachandran, R. Vesicle scission: dynamin. *Semin. Cell Dev. Biol.* **22**, 10–17 (2011).
16. Anantharam, A., Axelrod, D. & Holz, R. W. Real-time imaging of plasma membrane deformation reveals pre-fusion membrane curvature changes and a role for dynamin in the regulation of fusion pore expansion. *J. Neurochem.* **122**, 661–671 (2012).
17. Peters, C., Baars, T. L., Buhler, S. & Mayer, A. Mutual control of membrane fission and fusion proteins. *Cell* **119**, 667–678 (2004).
18. Ungermann, C., von Mollard, G. F., Jensen, O. N., Margolis, N., Stevens, T. H. & Wickner, W. Three v-SNAREs and two t-SNAREs, present in a pentameric cis-SNARE complex on isolated vacuoles, are essential for homotypic fusion. *J. Cell Biol.* **145**, 1435–1442 (1999).
19. Smaczynska-de, II R., Allwood, E. G., Aghamohammadzadeh, S., Hettema, E. H., Goldberg, M. W. & Ayscough, K. R. A role for the dynamin-like protein Vps1 during endocytosis in yeast. *J. Cell Sci.* **123**, 3496–3506 (2010).
20. Smaczynska-de, II R. *et al.* Yeast dynamin Vps1 and amphiphysin Rvs167 function together during endocytosis. *Traffic* **13**, 317–328 (2012).
21. Chappie, J. S., Acharya, S., Leonard, M., Schmid, S. L. & Dyda, F. G domain dimerization controls dynamin’s assembly-stimulated GTPase activity. *Nature* **27**, 435–440 (2010).
22. Mishra, R., Smaczynska-de, II R., Goldberg, M. W. & Ayscough, K. R. Expression of Vps1 I649K a self-assembly defective yeast dynamin, leads to formation of extended endocytic invaginations. *Commun. Integr. Biol.* **4**, 115–117 (2011).
23. Song, B. D., Yarar, D. & Schmid, S. L. An assembly-incompetent mutant establishes a requirement for dynamin self-assembly in clathrin-mediated endocytosis in vivo. *Mol. Biol. Cell* **15**, 2243–2252 (2004).
24. Collins, K. M., Thorngren, N. L., Fratti, R. A. & Wickner, W. T. Sec17p and HOPS, in distinct SNARE complexes, mediate SNARE complex disruption or assembly for fusion. *EMBO J.* **24**, 1775–1786 (2005).
25. Seals, D. F., Eitzen, G., Margolis, N., Wickner, W. T. & Price, A. A Ypt/Rab effector complex containing the Sec1 homolog Vps33p is required for homotypic vacuole fusion. *Proc. Natl Acad. Sci. USA* **97**, 9402–9407 (2000).
26. Alpadi, K. *et al.* Sequential analysis of trans-SNARE formation in intracellular membrane fusion. *PLoS Biol.* **10**, e1001243 (2012).
27. Kulkarni, A., Alpadi, K., Namjoshi, S. & Peters, C. A tethering complex dimer catalyzes trans-SNARE complex formation in intracellular membrane fusion. *Bioarchitecture* **1**, 59–69 (2012).
28. Macia, E., Ehrlich, M., Massol, R., Boucrot, E., Brunner, C. & Kirchhausen, T. Dynasore, a cell-permeable inhibitor of dynamin. *Dev. Cell* **10**, 839–850 (2006).
29. Collins, K. M. & Wickner, W. T. Trans-SNARE complex assembly and yeast vacuole membrane fusion. *Proc. Natl Acad. Sci. USA* **104**, 8755–8760 (2007).
30. Mohrmann, R. & Sørensen, J. B. SNARE requirements en route to exocytosis: from many to few. *J. Mol. Neurosci.* **48**, 387–394 (2012).
31. Scott, J. H. & Schekman, R. Lyticase: endoglucanase and protease activities that act together in yeast cell lysis. *J. Bacteriol.* **142**, 414–423 (1980).
32. Leonard, M., Song, B. D., Ramachandran, R. & Schmid, S. L. Robust colorimetric assays for dynamin’s basal and stimulated GTPase activities. *Methods Enzymol.* **404**, 490–503 (2005).

Acknowledgements

We thank Monique Reinhardt and Veronique Comte, University of Lausanne, and Swetha Mandalaju, Rice University, for their technical assistance. This study was supported by NIH grant GM087333 to C.P.; SNF 3100A0-128661/1 to A.M.; and NIH grant GM088803 and Welch Foundation (Q-581) to F.A.Q.

Author contributions

K.A. and C.P. designed research; K.A., A.K. and C.P. performed research; S.N., S.S., K.S., K.A., M.Z., A.S., A.M., M.E. and F.Q. contributed reagents; K.A. and C.P. wrote the manuscript.

Additional information

Supplementary Information accompanies this paper at <http://www.nature.com/naturecommunications>

Competing financial interests: The authors declare no competing financial interests.

Reprints and permission information is available online at <http://npg.nature.com/reprintsandpermissions/>

How to cite this article: Alpadi, K. *et al.* Dynamin–SNARE interactions control trans-SNARE formation in intracellular membrane fusion. *Nat. Commun.* **4**:1704 doi: 10.1038/ncomms2724 (2013).